Electronic Structure and Physical Characteristics of Dioxin Under External Electric Field

Wenyi Yin[1, 2], Xiangyun Zhang[1, 2, †], Bumaliya Abulimiti[3, *], Yuzhu Liu[1, 2, *], Yihui Yan[1, 2], Fengbin Zhou[1, 2] and Feng Jin[4]

Abstract: Dioxin is a highly toxic and caustic substance, which widely existed in the atmosphere, soil and water with tiny particles. Dioxin pollution has become a major problem that concerns the survival of mankind, which must be strictly controlled. The bond length, bond angle, energy, dipole moment, orbital energy level distribution of dioxin under the external field are investigated using DFT (density functional theory) on basis set level of B3LYP/6-31G (d, p). The results indicate that with the increase of the electric field, the length of one Carbon-Oxygen bond increases while another Carbon-Oxygen bond decreases. The energy gradually decreases with the electric field, while the change of the dipole moment has an opposite trend. In the infrared spectra, the vibration frequency decreases with the electric field increasing and shows an obvious red shift. Moreover, the ultraviolet-visible absorption spectra under different electric fields are analyzed with TD-DFT (time-dependent density functional theory) method. The wavelength of the strongest absorption peak increases and occurs red shift with the increase of the electric field. All the above results can provide reference for further research on the properties of dioxin under different external electric field.

Keywords: Dioxin, IR spectrum, UV-vis spectrum, electric field, density functional theory, excited states.

1 Introduction

Dioxin is a by-product of no use in industry as a single-ring organic compound. In recent years, dioxin has become the focus of the public. On the one hand, it can cause long-term damage to the body's metabolism and immunity. On the other hand, it has reproductive toxicity and genetic toxicity in addition to its carcinogenic toxicity, which directly

---

† Same contribution as the first author.

1 Jiangsu Key Laboratory for Optoelectronic Detection of Atmosphere and Ocean, Nanjing University of Information Science & Technology, Nanjing 210044, P. R. China.

2 Jiangsu Collaborative Innovation Center on Atmospheric Environment and Equipment Technology (CICAEET), Nanjing, 210044, P. R. China.

3 College of Physics and Electronic Engineering, Xinjiang Normal University, Urumqi 830054, P. R. China.

4 Advanced Technology Core, Baylor College of Medicine, Houston, TX 77030, USA.

* Corresponding author: Bumaliya Abulimiti. Email: maryam917@xjnu.edu.cn.
   Yuzhu Liu. Email: yuzhu.liu@gmail.com.

endangers the health and life of future generations [Yin, Li and Lu (2007); Castro, Soares and Vilarinho (2012); Taylor and Lenoir (2001)]. Therefore, dioxin pollution is a major problem that concerns the survival of mankind, which must be strictly controlled. Environmental experts say dioxin often exist in the atmosphere, soil and water with tiny particles, which main sources of pollution are chemical and metallurgical industry, waste incineration, paper making and pesticide production [Sun, Li and Li (2014)]. Since the Oile first reported that chlorine compounds in municipal waste and industrial waste may have produced dioxins during incineration in 1977, extensive research has been carried out [Olie, Vermeulen and Hutzinger (1977)]. The plastic bags used in daily life, and polyvinyl chloride soft glue and other things contain chlorine, which will release dioxins when they are burned and suspended in the air [Karasek and Dickson (1987); Zhang, Luo, Yin et al. (2016)]. The ground state structure, the physical and spectral characteristics of dioxin under different external electric fields are studied deeply, which will undoubtedly help us to understand the formation mechanism of dioxins and take some measures to avoid the harm to the environment. Therefore, the research on physical characteristics and spectrum of dioxin in the field is of great significance.

The physical and chemical properties of molecules will undergo a series of changes in the electric field, such as chemical bond breakage, the change of energy gap and absorption spectra [Yao, Xu, Liu et al. (2011); Xu, Yang, Lan et al. (2016); Xu and Liu (2010); Wu, Tan, Wan et al. (2013)]. The characterization of molecules under external electric fields has also become an important method for studying molecular properties. In recent years, it has been successfully applied in many fields that molecular characteristics are investigated under the external electric field [Cao, Zhou, Sun et al. (2018); Molina and Rowland (1974); Li, Liu, Yin et al. (2017); Mevel, Breger, Trainham et al. (1993); Zhang and Xie (2014)]. However, to our best knowledge, the effects of electric fields on dioxin have seldom been studied.

With the rapid development of computational science [Ren, Wang, Feng et al. (2018); Wang, Gu, Ma et al. (2016); Xia and Li (2017)], the physical and chemical properties of molecules under external electric fields can be calculated. Based on the geometric structure of dioxin under no electric field, in this paper, the influence of external electric field on the bond length, dipole moment, total energy and infrared spectrum of the dioxin is studied using the B3LYP/6-31G (d, p) method. And the ultraviolet-visible absorption spectra under different electric fields are analyzed using TD-DFT method.

2 Theoretical method

Under the external electric field, the Hamiltonian of the molecular system is shown as follows [Xu, Lv, Liu et al. (2009)]:

$$H = H_0 + H_{int} \tag{1}$$

Where H_0 is the Hamiltonian without electric field, H_{int} is the interaction Hamiltonian between molecules and electric field. Under the dipole approximately, it can be expressed as:

$$H_{int} = -\mu \cdot F \tag{2}$$

Where μ is the dipole moment of the molecule and F is the radiation field. The electric field discussed in this work is from 0 to 12 V/nm.

In the present work, the calculated results are obtained by using Gaussian 09 [Frisch, Trucks, Schlegel et al. (2009)]. The molecular structure of dioxin is optimized by using different methods and basis sets, based on density function theory. Compared with the experimental data, it is found that the bond length obtained with B3LYP /6-31G (d, p) basis set is in best agreement with the experimental results. The change of the bond length, the energy, the dipole moment, the infrared spectra, the ultraviolet-visible absorption spectra and dissociation properties of the molecule under different electric fields (0-12 V/nm) are studied on the basis set of B3LYP /6-31G (d, p).

3 Results and discussions

3.1 Molecular stability structure without the external electric field

In this paper, the configuration of dioxin is optimized with different methods and groups, and compared with the experimental data. The B3LYP/6-31G (d, p) method is more superior to the others in optimizing the structure of the dioxin. The optimized structure is shown in Fig. 1. The direction of the arrow is the direction of the electric field among them.
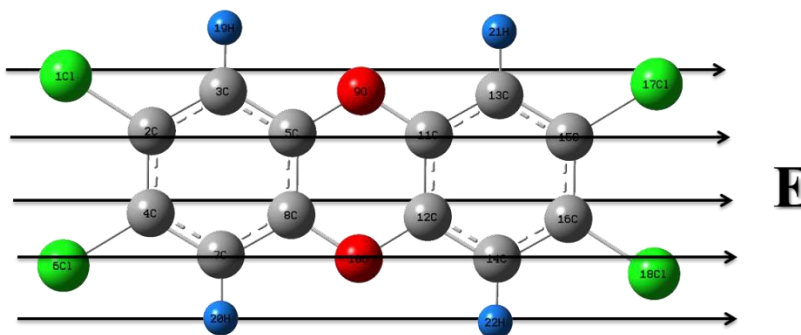

**Figure 1:** The optimized structure of dioxin at B3LYP/6-31G (d, p) level without electric field

3.2 Effect of external electric fields on bond length and total energy

Dioxins were optimized and calculated by the B3LYP/6-31G (d, p) method when different electric fields (0-12 V/nm) were applied. The stable structure of dioxins at different field strength was obtained. The calculated bond length (Carbon-Oxygen bond), bond angle (Carbon-Oxygen-Carbon) and dipole moment of the dioxins are given in Tab. 1. It can be seen from Tab. 1 that the total energy decreases gradually with the increase of the external electric field (0-12 V/nm), and the variation is shown in Fig. 2. The trend of Carbon-Oxygen bond of dioxin is shown in Fig. 3. The length of one Carbon-Oxygen bond increases gradually while another Carbon-Chlorine bond decreases with the increase of the electric field (0-12 V/nm). As is shown in Fig. 4, the bond angle (Carbon-Oxygen-Carbon) increases with the increase of the external electric field. The trend of the dipole moment is shown in Fig. 5. With gradually increasing the external field from 0-12 V/nm, the dipole moment increases.

Table 1: The calculated total energy, bond distances (Carbon-Oxygen), bond angle (Carbon-Oxygen-Carbon) and dipole moment of dioxin at different external electric fields

F(V/nm)	0	2	4	6	8	10	12
θ (°)	116.14079	116.18574	116.32325	116.56216	116.92323	117.42501	118.17426
R_{5C-9O} (Å)	1.37830	1.36947	1.36076	1.35222	1.34413	1.33641	1.33037
R_{11C-9O} (Å)	1.37830	1.38720	1.39610	1.40490	1.41348	1.42095	1.42622
μ (Debye)	0.00000	3.58880	7.22190	10.95110	14.85300	19.06390	23.90930
E (Hartree)	-2450.9007	-2450.9035	-2450.9120	-2450.9263	-2450.9466	-2450.9732	-2451.0069
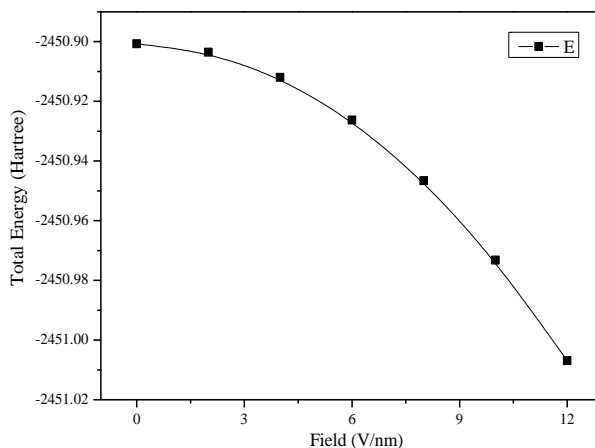
Figure 2: Variations of the total energy of dioxin under different electric fields (0-12 V/nm)
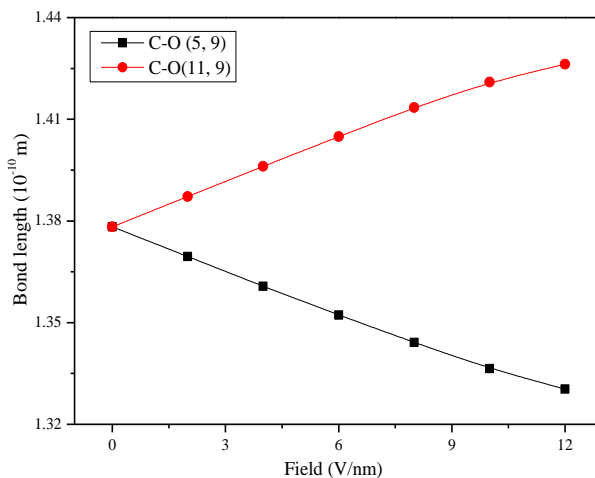
Figure 3: Variations of the bond length of Carbon-Oxygen bond with external electric field (0-12 V/nm)
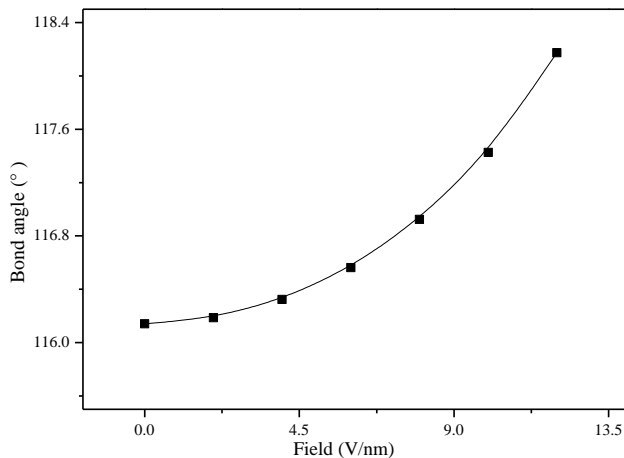
Figure 4: Variations of angle of Carbon-Oxygen-Carbon with external electric field (0-12 V/nm)
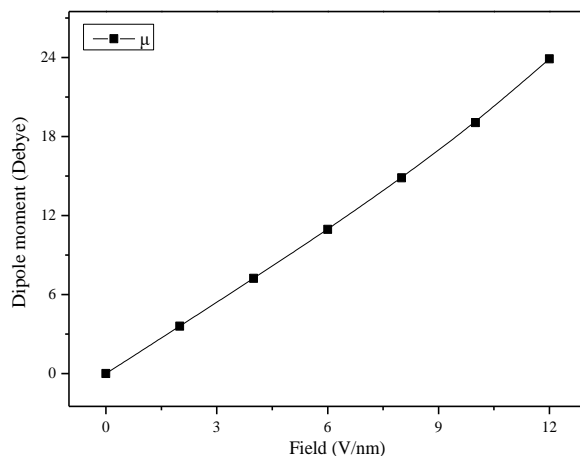
Figure 5: The changing tendency of the dipole moment under different electric fields (0-12 V/nm)

3.3 Effect of external electric fields on orbital energy level distribution

The energy of dioxin is calculated by using the same basis set. The lowest unoccupied molecule orbital (LUMO) energy E_L, the highest occupied molecule orbital (HOMO) energy E_H and the energy gap E_G of the dioxin under different electric fields (0-12 V/nm) are obtained, as is shown in Tab. 2. Where the energy gap E_G is calculated as follows:

$$E_G = (E_L - E_H) \times 27.2eV \tag{3}$$

The molecular LUMO energy is equivalent to molecular electron affinity. Moreover, when E_L is much lower, the molecule is easier to get the electrons. The molecule is easier to lose electrons when the E_H is high. E_G represents the ability of the transition from occupied orbit to unoccupied orbit. The changing tendency of E_L and E_H in the external

electric field are shown in Fig. 6. As can be seen from Fig. 6, E_H of the molecule increases slightly, and then linearly decreases approximately. The E_L decreases with the increase of electric field, but the trend is relatively slighter. The change of the molecular energy gap with the electric field is shown in Fig. 7. With the increase of the electric field, the energy gap decreases all the time. It illustrates that the electronic transitions from the lowest unoccupied molecule orbital (LUMO) to the highest occupied molecule orbital (HOMO) are much easier under electric field. It may cause a series of chemical changes.

Table 2: The calculated energy of the lowest unoccupied molecule orbital (LUMO) E_L, energy of the highest unoccupied molecule orbital (HOMO) E_H, and energy gap E_G for dioxin at different external fields

F (V/nm)	0	2	4	6	8	10	12
E_H (Hartree)	-0.22163	-0.21899	-0.21124	-0.19929	-0.18469	-0.16907	-0.15439
E_L (Hartree)	-0.04713	-0.05017	-0.05972	-0.08048	-0.10442	-0.12799	-0.15065
E_G (eV)	4.74640	4.59190	4.12134	3.23163	2.18334	1.11738	0.10173
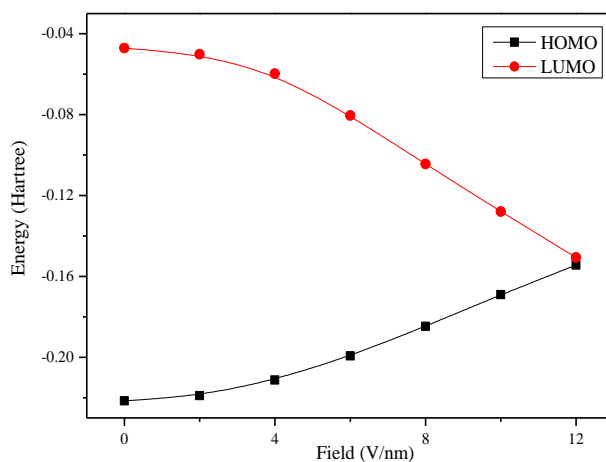
Figure 6: The changing tendency of highest occupied molecule orbital energy and lowest unoccupied molecular orbital energy with the external electric field varying from 0-12 V/nm
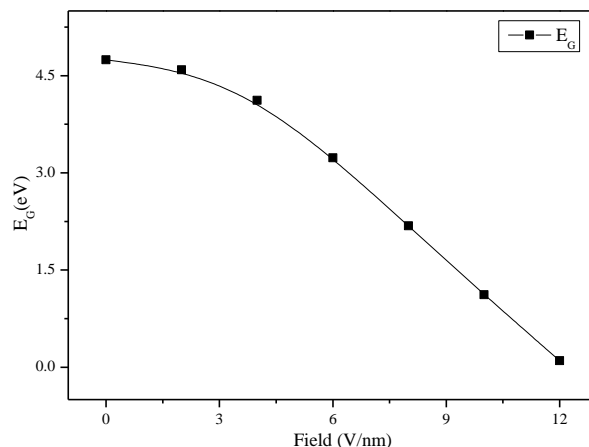
Figure 7: The relationship of energy gap under the external electric field (0-12 V/nm)

### 3.4 Effect of external electric fields on infrared spectra

The infrared spectrum can indicate some important physics or chemical properties, the dioxin was optimized and its infrared spectra were calculated by applying different intensity electric field (0-12 V/nm) at the B3LYP/6-31G (d, p) method. From the calculated results, sixty kinds of vibrational modes were obtained. In this paper, ten of them with the stronger strength are selected for analysis. The calculated vibrational frequencies and the corresponding vibration modes, including experimental values [Liu, Song, Yu et al. (2001)] are all listed in Tab. 3. Because the calculated and experimental values by non-Hartree-Fock method usually have a systematic error, and the usual way to avoid this is to multiply by a correction factor. Correction factors are slightly different for different methods and groups. This paper uses 0.9628 to correct the frequency in order for the vibration frequency to be consistent with the experimental value (1465cm^{-1}) at the maximum vibration intensity. The vibration frequency after correction is in good agreement with the experimental value.

Table 3: The calculated and experimental vibrational frequencies including the corresponding vibration modes

| v/cm^{-1}	v'/cm^{-1}	Experimental. v/cm^{-1}	Description
884	850.408	895	COC (system stretching)
899	864.838	916	COC (system stretching)
936	900.432	932	COC (system stretching)
1130	1087.06	1103	Ring breathing
1192	1146.704	1173	CCC (ring bending)
1260	1212.12	1248	CH (in plane deformation)
1320	1269.84	1306	COC (asym stretching)
1348	1296.776	1321	COC (asym stretching)
1518	1460.316	1465	Skeletal vibrations
1613	1551.706	1566	Skeletal vibrations

*v is the computed frequency and v' is the computed frequency scaled by 0.9628

Linear fitting theory is used to test if the computational infrared spectrum obtained by using DFT/B3LYP/6-31G (d, p) is in agreement with the standard experimental value. These two groups of peak frequencies in Tab. 3 are used as parameters in the linear least square method. The linear fitting result is shown in Fig. 8 and the correlation coefficient R^2 is 0.99815, which indicates that the computational infrared spectrum is in fair agreement with experimental value and the results illustrate the accuracy and reliability of the theoretical calculation.
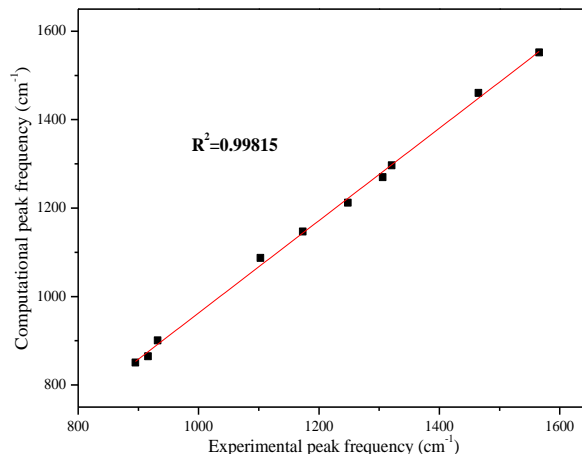
Figure 8: The linear fitting result of computational peak frequencies with experimental values

In this paper, these strong absorption peaks in the infrared spectra are analyzed, and the changing trends with the electric field are shown in Fig. 9. With the increase of the electric field, the vibration frequency gradually decreases, which shows a very obvious red shift phenomenon. In summary, the external electric field has a great influence on the infrared spectrum of dioxin and the effect of the external electric field on the different vibration modes is also significantly different.
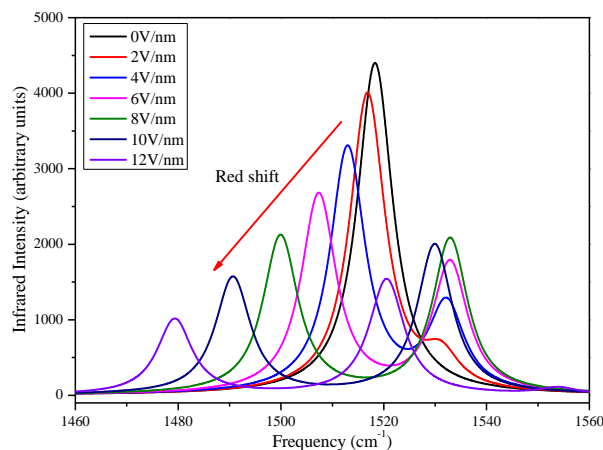
Figure 9: The variations of infrared spectrum of dioxin under external electric field (0-12 V/nm)

3.5 Effect of electric field on the ultraviolet-visible absorption spectra

The energy of the first fourteen excited states of dioxin is calculated at the basis set of 6-31G (d, p) using TD-DFT method. The ultraviolet-visible absorption spectrum of dioxin is obtained, and the absorption peak is at 216 nm. When the external field (0-12 V/nm) is applied, the changing trend of the spectra is shown in Fig. 10. The wavelength of the strongest absorption peak increases and occurs red shift with the increase of electric field.
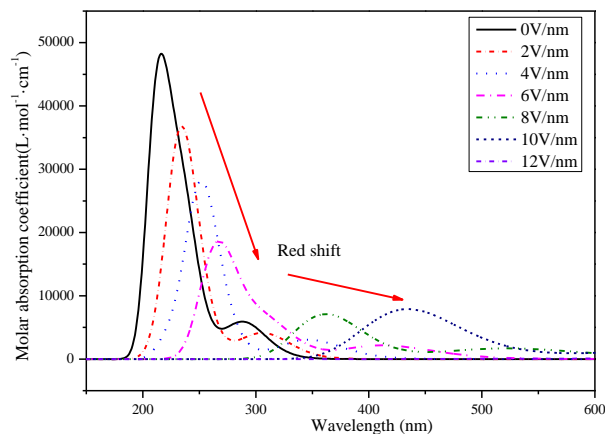
Figure 10: The ultraviolet-visible absorption spectra of dioxin under external electric field (0-12 V/nm)

In order to further analyze the excited properties of the molecule under the electric field, the oscillator strength *f* and the excited energy of the first 10 excited states under different electric fields are listed in Tab. 4 and Tab. 5. Oscillator strength *f* represents the electronic dipole transition probability. The transition is forbidden if oscillator strength *f* equals to zero. For example, the transition from the ground state to the first and second excited states cannot occur when *F* is from 10 to 12 V/nm, and so on. The oscillator strength *f* varies differently with the electric field, and the change is very complicated. The intensity of excited energy is shown in Tab. 5. The excitation energy of n= 3, 4, 7 excited states decreases with the change of the electric field, so the excited wavelength gradually increases and the dioxin is more likely to be excited. The excitation energy of other states changes without any rules with the increase of the electric field.

Table 4: The oscillator strength of first ten exited states of dioxin under electric fields

Field (V/nm)	n=1	2	3	4	5	6	7	8	9	10
0	0.0000	0.1444	0.0000	0.0001	0.0000	0.5714	0.0019	0.0000	0.0048	0.0000
2	0.0001	0.0979	0.0000	0.0144	0.0009	0.2806	0.0006	0.6410	0.0000	0.0000
4	0.0001	0.0748	0.0000	0.0232	0.0005	0.0000	0.1613	0.0002	0.5117	0.0170
6	0.0000	0.0535	0.0000	0.0000	0.0002	0.1381	0.0001	0.0000	0.0000	0.0000
8	0.0000	0.0413	0.0002	0.0000	0.0000	0.0001	0.0000	0.0001	0.1727	0.0032
10	0.0000	0.0000	0.0004	0.0373	0.0000	0.0000	0.0009	0.0002	0.0001	0.0000
12	0.0000	0.0000	0.0000	0.0005	0.0344	0.0000	0.0081	0.0000	0.0004	0.0000

Table 5: The excited energy of first ten excited states of dioxin under electric fields (unit: eV)

Field (V/nm)	n=1	2	3	4	5	6	7	8	9	10
0	4.0379	4.293	4.3941	4.8415	5.0192	5.2597	5.3226	5.4758	5.5532	5.6807
4	3.9092	4.0309	4.3646	4.4923	5.0763	5.0984	5.269	5.3264	5.33	5.415
8	3.5532	3.5753	3.6418	4.4099	4.4599	4.6253	4.8394	4.8426	4.9381	5.0163
12	2.7561	3.0026	3.0294	3.6779	3.828	3.9892	4.0926	4.3102	4.3647	4.5022
16	1.7583	2.3721	2.4002	2.6847	3.0581	3.2046	3.3389	3.3577	3.4223	3.5932
20	0.7163	1.6895	1.7369	1.7435	1.8503	2.2726	2.3908	2.6055	2.635	2.8252
24	-0.2956	0.7375	0.7437	1.1266	1.2116	1.2443	1.2921	1.9301	2.086	2.1254

4 Conclusions

In these works, the spectra and physical characteristics of dioxin under electric field are studied by density functional theory B3LYP/6-31G (d, p), including the bond length, bond angle, energy, dipole moment, the lowest unoccupied molecule orbital (LUMO) energy E_L and the highest occupied molecule orbital (HOMO) energy E_H and infrared spectra. In addition, the effect of the electric field on the ultraviolet-visible absorption spectra of the dioxin is analyzed adopting TD-DFT method. With the increase of the electric field, the length of one Carbon-Oxygen bond increases while another Carbon-Oxygen bond decreases. While the change of dipole moment has an opposite trend, the energy gradually decreases with the variety of the electric field. The energy gap gradually reduces as the electric field changes. The electron transitions from the lowest unoccupied molecule orbital (LUMO) to the highest occupied molecule orbital (HOMO) are more likely to happen. The electric field has an influence on the spectra of dioxin. In the infrared spectra, the vibration frequency decreases with the electric field increasing and shows an obvious red shift phenomenon. Additionally, the ultraviolet-visible absorption spectra have changed under electric field. The wavelength of the strongest absorption peak increases and occurs red shift with the increase of the electric field. Research on physical characteristics and spectrum of dioxin in the field is of great significance and it is expected to give more physical evidence and references for spectroscopist as well as environmentalist.

References

Cao, Y.; Zhou, Z.; Sun, X.; Gao, C. (2018): Coverless information hiding based on the molecular structure images of material. *Computers, Materials & Continua,* vol. 54, no. 2, pp. 197-207.

Castro, A.; Soares, D.; Vilarinho, C. (2012): Kinetics of thermal de-chlorination of PVC under pyrolytic conditions. *Waste Management*, vol. 32, no. 5, pp. 847-851.

Frisch, M. J.; Trucks, G. W. ; Schlegel, H. B. (2009): *Gaussian 09,* revision D. 01. Wallingford CT: Gaussian Inc.

Karasek, F. W.; Dickson, L. C. (1987): Model studies of polychlorinated dibenzo-p-dioxin formation during municipal refuse incineration. *Science*, vol. 237, no. 4816, pp. 754-756.

Li, J.; Liu, Y.; Yin, W.; Zhang, X. (2017): Spectra and dissociation properties of Freon 31 under electric field. *Spectroscopy Letters*, vol. 50, no. 10, pp. 572-578.

Liu, G.; Song, X.; Yu, J.; Qian, X. (2001): Theoretical studies on the structure and thermodynamic properties of 2,3,7,8-tetrachlorinated dibenzo-p-dioxin. *Chinese Journal of Chemical Physics*, vol. 14, no. 4, pp. 414-420.

Mevel, E.; Breger, P.; Trainham, R. (1993): Atoms in strong optical fields: Evolution from multiphoton to tunnel ionization. *Physical Review Letters*, vol. 70, no. 4, pp. 406-409.

Molina, M. J.; Rowland, F. S. (1974): Stratospheric sink for cholofluoromethanes: Chlorine atom-catalysed destruction of ozone. *Nature,* vol. 249, no. 5460, pp. 810-812.

Olie, K.; Vermeulen, P. L.; Hutzinger, O. (1977): Chlorodibenzo-pdioxins and chlorodi-benzofurans are trace components of fly ash and flue gas of some municipal incinerators in the Netherlands. *Chemosphere*, vol. 6, no. 8, pp. 445-459.

Ren, Y.; Wang, J.; Feng, X.; Younn, G.; Kim, J. U. (2018): A hierarchical clustering based method to evaluate reuse of rare earth tailings under cloud computing environment. *Cluster Computing*, pp. 1-10.

Sun, J.; Li, Q. H.; Li, G. X. (2014): Experimental and thermodynamic investigation on partitioning and speciation of NaCl during municipal solid waste incineration. *Proceedings of the CSEE*, vol. 34, no. 2, pp. 272-278.

Taylor, P. H.; Lenoir, D. (2001): Chloroaromatic formation in incineration processes. *Science of the Total Environment*, vol. 269, no. 1-3, pp. 1-24.

Wang, B.; Gu, X.; Ma, L.; Yan, S. (2017): Temperature error correction based on BP neural network in meteorological wireless sensor network. *International Journal of Sensor Networks*, vol. 23, no. 4, pp. 265-278.

Wu, D.; Tan, B.; Wan, H.; Zhang, X.; Xie, A. (2013): Molecular properties and potential energy function model of BH under external electric field. *Chinese Physics B*, vol. 22, no. 12, pp. 123101: 1-5.

Xia, Z.; Li, X. (2017): Coverless information hiding method based on LSB of the character. *Journal of Internet technology*, vol. 18, no. 6, pp. 1353-1360.

Xu, G.; Liu, X. (2010): Si_2O_2 molecule: Structure of ground state and the excited properties under different external electric fields. *Chinese Physics B*, vol. 19, no. 11, pp. 113101: 1-5.

Xu, G.; Lv, W.; Liu, Y. (2009): Effect of external electric field on the optical excitation of silicon dioxide. *Acta Physica Sinica*, vol. 58, no. 5, pp. 3058-3063.

Xu, W.; Yang, G.; Lan, P.; Ma, H. (2016): Excluded volumes of anisotropic convex particles in heterogeneous media: Theoretical and numerical studies. *Computers, Materials & Continua*, vol. 52, no. 1, pp. 25-40.

Yao, D.; Xu, G.; Liu, X. (2011): Study of the excitation properties of the Si_3O_2 cluster under an external electric field. *Chinese Physics B*, vol. 20, no. 10, pp. 103101: 1-5.

Yin, X.; Li, X.; Lu, S. (2007): On-line real-time monitoring of trace organic pollutant formation in the simulated flue gas. *Proceedings of the CSEE*, vol. 27, no. 17, pp. 29-33.

Zhang, G.; Xie, S. (2014): Temperature and electric field effect on proton transfer in adenine-thymine. *Bulletin of the Korean Chemical Society*, vol. 35, no. 12, pp. 3532-3534.

Zhang, R.; Luo, Y.; Yin, R. (2016): Experimental study on the inhibition effect of H_2 on dioxin emission in MSW gasification. *Proceedings of the CSEE*, vol. 36, no. 8, pp. 2195-2201.